Vol 16 No 1, January 2007
1009-1963/2007/16(01)/0249-09

Chinese Physics

© 2007 Chin. Phys. Soc.
and IOP Publishing Ltd

Controlling optical responses through local dielectric resonance in nanometre metallic clusters*

Chen Liang-Liang(陈亮亮), Gu Ying(古 英)†, Wang Li-Jin(王立金), and Gong Qi-Huang(龚旗煌)‡

State Key Laboratory for Mesoscopic Physics, School of Physics, Peking University, Beijing 100871, *China*

(Received 2 June 2006; revised manuscript received 2 August 2006)

Optical responses in dilute composites are controlled through the local dielectric resonance of metallic clusters. We consider two located metallic clusters close to each other with admittances ε_1 and ε_2. Through varying the difference admittance ratio $\eta[=(\varepsilon_2-\varepsilon_0)/(\varepsilon_1-\varepsilon_0)]$, we find that their optical responses are determined by the local resonance. There is a blueshift of absorption peaks with the increase of η. Simultaneously, it is known that the absorption peaks will be redshifted by enlarging the cluster size. By adjusting the nano-metallic cluster geometry, size and admittances, we can control the positions and intensities of absorption peaks effectively. We have also deduced the effective linear optical responses of three-component composites $\varepsilon_{\rm e}=\varepsilon_0\big(1+\sum_{n=1}^{n_{\rm s}}[(\gamma_{n_1}+\eta\gamma_{n_2})/(\varepsilon_0(s-s_n))]\big)$, and the sum rule of cross sections: $\sum_{n=1}^{n_{\rm s}}(\gamma_{n_1}+\eta\gamma_{n_2})=N_{h_1}+N_{h_2}$, where $N_{h_1}$and N_{h_2} are the numbers of ε_1 and ε_2 bonds along the electric field, respectively. These results may be beneficial to the study of surface plasmon resonances on a nanometre scale.

Keywords: local dielectric resonance, effective linear optical response, nanometre metallic cluster
PACC: 7430G, 8160H

1. Introduction

Optical properties of composites composed of many nanometre metallic clusters have attracted great interest. Due to simultaneous existence of the positive and negative dielectric constants in these composites, in the quasistatic limit, dielectric resonances may occur accompanying the very localized field distribution within and around the metallic clusters.[1−3] It is known that the localized excitation on roughly nanostructured surfaces,[4] the surface-plasmon modes in disordered nanosystems,[5−7] and the selective photomodification in fractal aggregates of metallic colloidal particles,[8] are highly sensitive to the local-field distribution, which is related to the specific resonance mode. The field confinement at the quasistatic resonances is several orders of magnitude larger around the nano-scale metallic particle and thus will cause locally increased exposure of thin layer of photoresists, which may provide the nanolithography without diffraction limit.[9,10] The localization of electric field can also lead to dramatic enhancement of linear and nonlinear optical responses.[11−16]

For these potential applications, Green's function formalism (GFF) was developed to study the dielectric resonance properties of metallic clusters embedded in the dielectric host.[3,4,17] Using the GFF, the local field distribution near resonances can be computed, so the effective linear and nonlinear optical responses can be directly obtained. In this connection, optical responses of various composites are investigated. In the dilute anisotropic composites, the separation and overlap of the absorption peaks and third-order nonlinear enhancement peaks were reported.[11] For 2D and 3D disordered composites, the absorption range was found broadened with increasing impurity concentration, while a redshift of the absorption peak was observed only in 3D region.[4] In the composites containing periodical or random metallic cells, optical responses were determined through the mechanism of local dielectric resonance of a single metallic cell.[12,14] In addition, in fractal structured composites, optical responses exhibited the similar distribution with increasing fractal level.[13] The main goal of this paper is to investigate how to control the optical responses of dielectric-metallic composites on a nanometre scale.

*Project supported by the National Natural Science Foundation of China(Grant Nos 10304001, 10334010, 10521002, 10434020, 10328407 and 90501007).
†E-mail: ygu@phu.edu.cn
‡E-mail: qhgong@pku.edu.cn

The paper is organized as follows. In Section 2, the effective linear optical response in a three-component composite with admittances ε_0 (dielectric host), ε_1 (metal) and ε_2 (varied as $\eta[=(\varepsilon_2-\varepsilon_0)/(\varepsilon_1-\varepsilon_0)]$) is deduced and expressed as

$$\varepsilon_{\rm e}=\varepsilon_0\Big(1-\sum_{n=1}^{n_{\rm s}}\frac{\gamma_n}{(s-s_n)}\Big)$$

in the lattice model. The cross section γ_n in a uniform electric field is proved obeying the sum rule: $\sum_{n=1}^{n_{\rm s}}\gamma_n=N_{h_1}+\eta N_{h_2}$, where N_{h_1} and N_{h_2} are the numbers of ε_1 and ε_2 bonds along the field respectively. In Section 3, the cross sections of various single metallic clusters are summarized for the use in controlling the optical responses. In this paper we will show how to control the optical responses through the local resonances of metallic clusters. Then in Section 4, as an example, we consider two close-located metallic clusters with admittances ε_1 and ε_2. By varying $\eta[=(\varepsilon_2-\varepsilon_0)/(\varepsilon_1-\varepsilon_0)]$, we find that their optical responses are determined by the local resonance. There is a blueshift of absorption peaks with the increase of the difference admittance ratio η. Meanwhile, we also show that the absorption peaks will be redshifted by enlarging the cluster size. So by adjusting the nanometallic clusters geometry, size and admittances, we can control the positions and intensities of absorption peaks effectively. Finally we summarize the main results in the last section. These results may be beneficial to the study of surface plasmon resonances on a nanometre scale.

2. Effective linear optical response of three-component composite

The effective linear and nonlinear optical responses in the binary composites have been obtained.[11] Now we consider an infinite three-component composite network. As shown in Fig.1,[17] where the impurity bonds with admittances ε_1 and ε_2 are employed to replace the bonds in an otherwise homogeneous network of identical admittance ε_0. The admittance of each metallic bond is generally complex and frequency-dependent. We always use $\eta=(\varepsilon_2-\varepsilon_0)/(\varepsilon_1-\varepsilon_0)$ to express ε_2. The impurity bonds construct the clusters subspaces S_1 and S_2, while the bonds in the dielectric host belongs to S_0. The whole space is $S=S_0\cup S_1\cup S_2$. Among ε_1, ε_2 and ε_0, there must exist at least one negative value if dielectric resonance happens. GFF can be used to obtain the dielectric resonances and the local field distributions near resonances.[17] Green's matrix in the clusters subspace is defined as

$$\tilde{M}=\sum_{\boldsymbol{y}\in S_1(\boldsymbol{z})}(G_{\boldsymbol{x},\boldsymbol{z}}-G_{\boldsymbol{x},\boldsymbol{y}})+\eta\sum_{\boldsymbol{y}\in S_2(\boldsymbol{z})}(G_{\boldsymbol{x},\boldsymbol{z}}-G_{\boldsymbol{x},\boldsymbol{y}}).$$

The nontrivial eigenvalues $s(=1/(1-\varepsilon_1/\varepsilon_0))$ of $\tilde{M}$ construct the dielectric resonance spectrum. $\tilde{R}_m$ and $\tilde{L}_m$ are the mth normalized right and left eigenvectors of $\tilde{M}$. Near resonances, the electric fields are localized within and around the metallic clusters. In the uniform field $E_0(=1)$ along $\mathbf{1}$ direction, we can compute the electrical potential of point $\boldsymbol{x}$:[17]

$$V_{\boldsymbol{x}}=\boldsymbol{x}_1+\sum_{n=1}^{n_{\rm s}}\frac{s}{(s-s_n)}\times\sum_{\boldsymbol{y}\in\boldsymbol{C}}\tilde{L}_{n,\boldsymbol{y}}\boldsymbol{y}_1\sum_{\boldsymbol{z}\in\boldsymbol{C}}M_{\boldsymbol{x},\boldsymbol{z}}\tilde{R}_{n,\boldsymbol{z}},\qquad(1)$$

where

$$M_{\boldsymbol{x},\boldsymbol{z}}=\sum_{\boldsymbol{y}\in S_1(\boldsymbol{z})}(G_{\boldsymbol{x},\boldsymbol{z}}-G_{\boldsymbol{x},\boldsymbol{y}})+\eta\sum_{\boldsymbol{y}\in S_2(\boldsymbol{z})}(G_{\boldsymbol{x},\boldsymbol{z}}-G_{\boldsymbol{x},\boldsymbol{y}}),$$

which is different from the $\tilde{M}$ matrix above.

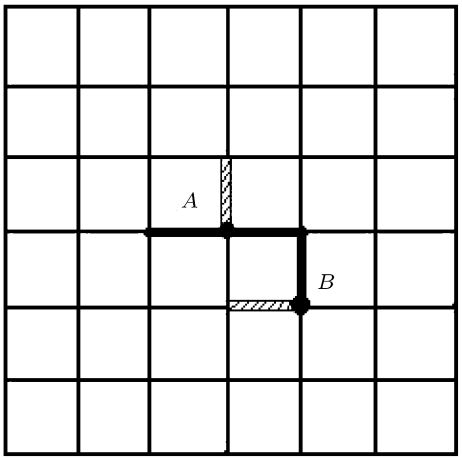


Fig.1. Schematic diagram of a metallic cluster (shown in thick lines) embedded in a two dimensional dielectric network.[17] The shadowed bonds have the admittance ε_2.

In the continuum, the effective dielectric constant $\varepsilon_{\rm e}$ in 2D region is defined as[18]

$$\varepsilon_{\rm e}=\frac{1}{S}\int_S{\rm d}s\varepsilon(\boldsymbol{r})\frac{\boldsymbol{E}_0\cdot\boldsymbol{E}(\boldsymbol{r})}{E_0^2},\qquad(2)$$

where S stands for the area of the composite, and $\varepsilon(\boldsymbol{r})$ and $\boldsymbol{E}(\boldsymbol{r})$ are the admittance and local electric field at point $\boldsymbol{r}$. For a three-component composite it reads

$$\varepsilon_{\rm e}=\frac{1}{S}\Big(\int_{S_0}{\rm d}s\varepsilon_0\frac{\boldsymbol{E}_0\cdot\boldsymbol{E}(\boldsymbol{r})}{E_0^2}+\int_{S_1}{\rm d}s\varepsilon_1\frac{\boldsymbol{E}_0\cdot\boldsymbol{E}(\boldsymbol{r})}{E_0^2}+\int_{S_2}{\rm d}s\varepsilon_2\frac{\boldsymbol{E}_0\cdot\boldsymbol{E}(\boldsymbol{r})}{E_0^2}\Big),\tag{3}$$

with $S=S_0\cup S_1\cup S_2$. By some transformation

$$\varepsilon_{\rm e}=\frac{1}{S}\Big(\int_{S}{\rm d}S\varepsilon_0\frac{\boldsymbol{E}_0\cdot\boldsymbol{E}(\boldsymbol{r})}{E_0^2}+\int_{S_1}{\rm d}s(\varepsilon_1-\varepsilon_0)\frac{\boldsymbol{E}_0\cdot\boldsymbol{E}(\boldsymbol{r})}{E_0^2}+\int_{S_2}{\rm d}s(\varepsilon_2-\varepsilon_0)\frac{\boldsymbol{E}_0\cdot\boldsymbol{E}(\boldsymbol{r})}{E_0^2}\Big),\tag{4}$$

and normalization $\boldsymbol{E}_0=\frac{1}{S}\int_S{\rm d}s\boldsymbol{E}(\boldsymbol{r})$, $\varepsilon_{\rm e}$ becomes

$$\varepsilon_{\rm e}=\varepsilon_0+\frac{1}{S}\Big(\int_{S_1}{\rm d}s(\varepsilon_1-\varepsilon_0)\frac{\boldsymbol{E}_0\cdot\boldsymbol{E}(\boldsymbol{r})}{E_0^2}+\int_{S_2}{\rm d}s(\varepsilon_2-\varepsilon_0)\frac{\boldsymbol{E}_0\cdot\boldsymbol{E}(\boldsymbol{r})}{E_0^2}\Big).\tag{5}$$

Setting $S=1$ and $E_0=1$, we can rewrite it as

$$\varepsilon_{\rm e}=\varepsilon_0+\int_{S_1}{\rm d}s(\varepsilon_1-\varepsilon_0)\boldsymbol{E}(\boldsymbol{r})_{//}+\int_{S_2}{\rm d}s(\varepsilon_2-\varepsilon_0)\boldsymbol{E}(\boldsymbol{r})_{//},\tag{6}$$

where $\boldsymbol{E}(\boldsymbol{r})_{//}$ stands for the part of $\boldsymbol{E}(\boldsymbol{r})$ parallel to the incident field along **1** direction. Then in the lattice model we have

$$\varepsilon_{\rm e}=\varepsilon_0\Big(1+\sum_{(\boldsymbol{x},\boldsymbol{y})\in S_1}\frac{(\varepsilon_1-\varepsilon_0)}{\varepsilon_0}(V_{\boldsymbol{x}}-V_{\boldsymbol{y}})(\boldsymbol{x}_1-\boldsymbol{y}_1)+\eta\sum_{(\boldsymbol{x}',\boldsymbol{y}')\in S_2}\frac{(\varepsilon_1-\varepsilon_0)}{\varepsilon_0}(V_{\boldsymbol{x}'}-V_{\boldsymbol{y}'})(\boldsymbol{x}'_1-\boldsymbol{y}'_1)\Big).\tag{7}$$

By introducing

$$\gamma_{n_1}=\Big(\sum_{\boldsymbol{y}\in S}\tilde{L}_{n,\boldsymbol{y}\boldsymbol{y}_1}\Big)\times\sum_{(\boldsymbol{x},\boldsymbol{y})\in S_1}(\boldsymbol{x}_1-\boldsymbol{y}_1)(\tilde{R}_{n,\boldsymbol{x}}-\tilde{R}_{n,\boldsymbol{y}}),$$

and

$$\gamma_{n_2}=\Big(\sum_{\boldsymbol{y}\in S}\tilde{L}_{n,\boldsymbol{y}\boldsymbol{y}_1}\Big)\times\sum_{(\boldsymbol{x},y)\in S_2}(\boldsymbol{x}_1-\boldsymbol{y}_1)(\tilde{R}_{n,\boldsymbol{x}}-\tilde{R}_{n,\boldsymbol{y}}),$$

the effective linear optical response $\varepsilon_{\rm e}$ of a three-component composite is simplified,

$$\varepsilon_{\rm e}=\varepsilon_0\Big(1-\sum_{n=1}^{n_{\rm s}}\frac{\gamma_n}{(s-s_n)}\Big),\tag{8}$$

with the cross section $\gamma_n=\gamma_{n_1}+\eta\gamma_{n_2}$, which represents the intensity of optical response for resonance s_n. The imaginary part of $\varepsilon_{\rm e}$ is corresponding to the absorption

$$-{\rm Im}(\varepsilon_{\rm e})={\rm Im}\sum_{n=1}^{n_{\rm s}}\frac{\gamma_n}{(s-s_n)}.\tag{9}$$

We now prove the sum rule of the cross sections for a three-component composite. From Eq.(3), in $2D$ composite, $m(h_i)$ with $h_i=(\varepsilon_i/\varepsilon_0)(i=1,2)$ is written as[19]

$$m(h_1)\equiv\frac{\varepsilon_{\rm e}}{\varepsilon_0}=\frac{1}{S}\boldsymbol{E}_0\int_S(\theta_1h_1+\theta_2h_2+\theta_0)\frac{\boldsymbol{E}(\boldsymbol{r})}{E_0^2}{\rm d}s\tag{10}$$

$$=\frac{1}{S}\boldsymbol{E}_0\int_S(\theta_1h_1+\theta_2(\eta h_1+(1-\eta))+\theta_0)\frac{\boldsymbol{E}(\boldsymbol{r})}{E_0^2}{\rm d}s,\tag{11}$$

where $\theta_i(\boldsymbol{r})=1$ if $\boldsymbol{r}$ is inside the ith component while $\theta_i(\boldsymbol{r})=0$ if $\boldsymbol{r}$ is outside that component.[19] The first derivative of $m(h_1)$ is

$$\frac{\partial m(h_1)}{\partial h_1}=\frac{1}{S}\boldsymbol{E}_0\int_S(\theta_1+\eta\theta_2)\frac{\boldsymbol{E}(\boldsymbol{r})}{E_0^2}{\rm d}s\tag{12}$$

$$=\frac{1}{S}E_0\int_S(\theta_{1_{//}}+\eta\theta_{2_{//}})\frac{E_0}{E_0^2}{\rm d}s,\tag{13}$$

and its discrete form is

$$\frac{\partial m(h_1)}{\partial h_1}=\frac{1}{S}\sum_S(\theta_{1_{//}}+\eta\theta_{2_{//}})\Delta x\Delta y$$

$$=N_{h_1}+\eta N_{h_2},\tag{14}$$

where $S=1$, and N_{h_1} is the number of ε_1 bonds along the field and N_{h_2} the number of ε_2 bonds along the field. On the other hand, we can calculate the first derivative of $m(h_1)$ from $\varepsilon_{\rm e}$ obtained in Eq.(8):

$$m'(h_1)\mid_{h_1=1}=\Big(1-\sum_{n=1}^{n_{\rm s}}\frac{\gamma_{n_1}+\eta\gamma_{n_2}}{(s-s_n)}\Big)'\Big|_{h_1=1}$$

$$= \sum_{n=1}^{n_s} \gamma_{n_1} + \eta\gamma_{n_2}, \tag{15}$$

in this function $s = \varepsilon_0/(\varepsilon_0 - \varepsilon_1) = 1/(1 - h_1)$.[19] Comparing Eq.(14) with Eq.(15), we obtain the sum rule:

$$\sum_{n=1}^{n_i} \gamma_n = \sum_{n=1}^{n_i} (\gamma_{n_1} + \eta\gamma_{n_2}) = N_{h_1} + \eta N_{h_2}. \tag{16}$$

Note that in a three-component composite the sum of the cross section areas is in proportion to difference admittance ratio η (instead of being proportional to the admittance ε_2), which will contribute more to the optical responses when η is positive and large. When $\eta = 1$, the composite is back to the binary case:[11]

$$\varepsilon_e = \varepsilon_0 \Big(1 - \sum_{n=1}^{n_s} \frac{\gamma_n}{(s - s_n)}\Big), \tag{17}$$

and the sum rule reverts to $\sum_{n=1}^{n_i} \gamma_n = N_h$,[11] where N_h is the number of horizontal bonds along the applied field. These sum rules are also proved by the numerical calculations.

3. Optical responses of small metallic clusters

It is known that in the dilute composites most of the impurity clusters (also called lattice animals[20]) only have a few connected metallic bonds. The optical responses of dilute composites are determined by the local resonance mechanism of these lattice animals,[20] while the ambient animals have only a little influence on the optical properties. In this section, as a preparation, we compute the cross section areas of optical responses for the resonances of 1-bond, 2-bond, and 3-bond metallic clusters, as shown in Fig.2. Since these cross section areas to some degree represent the intensities of optical responses, they are instructive to the design of the optical responses of dilute composites containing many lattice animals.

Table 1 lists the nonzero cross section γ_n of each resonance s_n for various lattice animals in Fig.2. The uniform electric field is along the horizontal direction. From the table, we see that the optical responses of these lattice animals are distributed within the area $s \in (0.25, 0.8)$. For the typical metal plasma frequency $\omega_p \sim 10^{16}$ and the water parameter $\varepsilon_0 = 1.77$, they correspond to the wavelength region from infrared 1600 nm to visible 760 nm. The parameters of these lattice animals are instructive to the design of the optical responses of dilute composites. For example, if we want to design large optical responses at $s = 0.5$, the geometric structures 11, 321, and 322 are more likely to be chosen. And if we desire to have the optical responses in the infrared region such as $s = 0.25$(1600 nm), the geometric structures 311, 321, 341, and 342 may be chosen. For the same lattice animal, the larger cross section values always correspond to the stronger optical responses, and the summation of cross sections obeys the sum rule:

$$\sum_n \gamma_n = N_h.$$

For the geometric structures 221, 322, 341, 342, they have almost the comparable strength in optical responses for each resonance; while, for other geometric structures 311, 321, 331, 352, there are the obvious differences in the strengths of the optical responses. The above viewpoints are helpful to the design of the required optical responses in dilute binary composites.

Table 1. The nonzero cross section γ_n of each resonance S_n for various lattice animals.

Clusters geometry	Resonances S_n	Cross sections γ_n
11	0.50000	1.00000
211	0.36338	2.00000
221	0.68169	0.50000
	0.31831	0.50000
311	0.67136	0.03620
	0.28216	2.96380
321	0.70714	0.14062
	0.54316	0.55553
	0.24970	1.30384
322	0.70714	0.32317
	0.54316	0.34918
	0.24970	0.32765
331	0.69756	0.62846
	0.16582	0.37154
332	0.63662	2.00000
341	0.75695	1.00000
	0.24305	1.00000
342	0.75695	0.50000
	0.24305	0.50000
351	0.36338	2.00000
352	0.83418	0.37154
	0.30244	0.62846

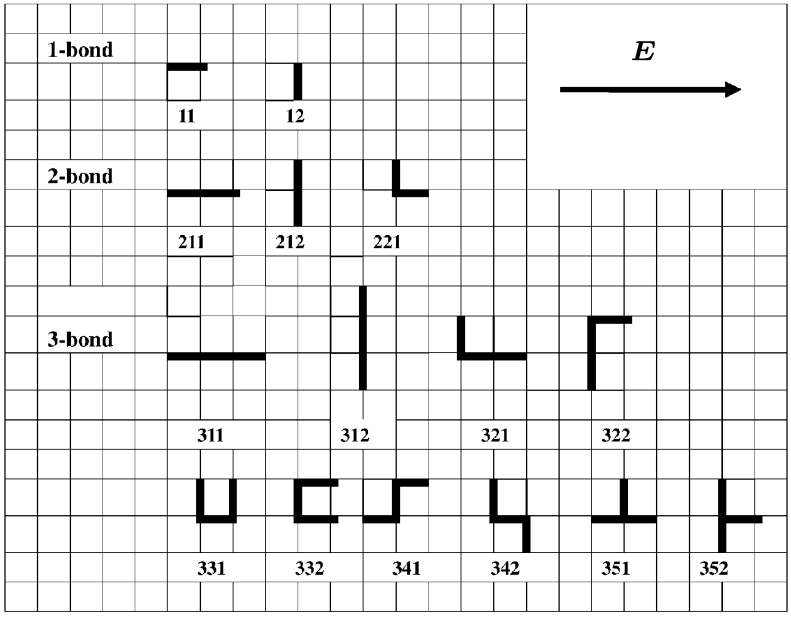


Fig.2. Schematic diagram of various 1-bond, 2-bond, and 3-bond metallic clusters (shown in thick lines). The applied field is along the horizontal direction.

4. Controlling optical responses through local resonance

In periodical or randomly arrayed metallic cells, it has been known that the microstructure of a single cell determines the optical responses of the whole composite.[12,14] By introducing defects into the cells, we have found that the optical responses are modified according to the single-cell responses, called the local resonance. Here we want to know the difference among the optical responses if there exist metallic clusters with different admittances in the composite. As an example, consider two metallic clusters with the same geometry, but with different admittances, as shown in the insets in Figs.3 and 4. The Drude free electron model is employed here to compute the optical properties. The admittance ε_1 of the impurity metallic bonds in cluster 1 is defined as $\varepsilon_1(\omega) = 1 - \omega_p^2/\omega(\omega + \mathrm{i}\gamma)$, where $\omega_p \approx 10^{16}$ is the plasma frequency, $\gamma = 0.01\omega_\mathrm{p}$ is a damping constant and $\varepsilon_0 = 1.77$. The admittance of cluster 2 is varied according to $\varepsilon_2 = \varepsilon_0 + \eta(\varepsilon_1 - \varepsilon_0)$[17] with the admittance ε_1 of cluster 1. It is found that the local resonances determine the positions and intensities of the optical responses, while the clusters in the ambience have a weak modulation to the optical responses.

In order to eliminate the influence of the ambience, we first investigate the optical responses of two clusters separated by a large distance $d = 10$. Figure 3 displays the imaginary part of the effective linear optical responses ε_e of two isolated metallic clusters (inset in Fig.3(a)) when η is varied from -1.0 to 2.0. Here s is the real part of

$$s = \frac{1}{1 - \varepsilon_1(\omega)/\varepsilon_0}$$

and the absolute value of s is increased with ω monotonically. For $\eta = 1.0$ in Fig.3(c), the two clusters are identical. They are separated far from each other and there is no obvious coupling between them, so the positions and intensities of absorption peaks are the same as that found when only one cluster exists, i.e., $s_1 = 0.23556$, $s_2 = 0.31254$, and $s_3 = 0.59706$. When $\eta = -1.0$ in Fig.3(a), for $s \in [0, 1]$, $\varepsilon_2 > 0$, cluster 2 has no metallic component, so it has no contribution to the optical responses. Then η is increased to 0.2 in Fig.3(b), and the metallic component of cluster 2 appears, showing the small peaks in the infrared region. In this case, cluster 2 has a little contribution to the main absorption peaks. When $\eta > 1$, ε_2 has a larger negative real part than ε_1, and leads to three new absorption peaks s_4, s_5, and s_6, as shown in Fig. 3(e). When $\eta = 1.3$, peaks s_2 and s_4 overlap each

other, leading to the enhancement of optical responses at $s_2 = 0.31254$ in Fig. 3(d). When η increases to 1.6 in Fig.3(e), the peaks s_4, s_5, and s_6 are blueshifted and the intensity of s_4 exceeds that of s_2, while the positions of peaks s_1, s_2, and s_3 are almost fixed. As η increases to $\eta > 2.0$, we find that the peak s_4 keeps blueshifted and enhanced, and the peak s_6 moves out of the frequency region. The reason of enhancing s_4 peak is that the metallic component of cluster 2 become stronger or the negative real part of ε_2 becomes larger. From the figure, we find that the optical responses are determined by the local resonances of the two metallic clusters, and can be effectively controlled by modulating η.

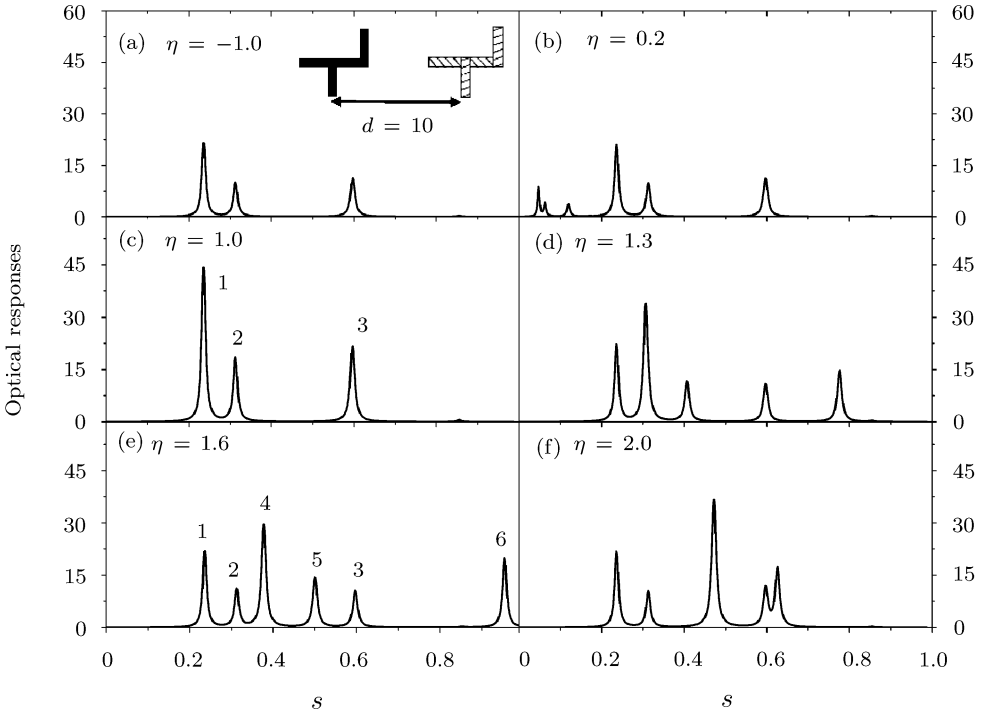


Fig.3. Optical responses of two separate clusters with the distance $d = 10$. (a) $\eta = -1.0$, (b) $\eta = 0.2$, (c) $\eta = 1.0$, (d) $\eta = 1.3$, (e) $\eta = 1.6$, and (f) $\eta = 2.0$.

In real composites, the ambient perturbation to the optical responses is not negligible. For simplicity we only consider two closely situated clusters. Figure 4 displays the imaginary part of ε_e of two isolated metallic clusters separated by a distance $d = 3$ (the inset in Fig.4(a)) when η is varied from -1.0 to 2.0. It is seen that in Fig.4(c), due to the perturbation between clusters, there are slight differences in positions and intensities of absorption peaks from those found for a single cluster. Then in Figs.4(a) and 4(b), for the same reason mentioned above, i.e. the admittance of the metallic component of cluster 2 is not large enough and thus has little contribution to the optical properties, only three main absorption peaks are observed. When $\eta = 1.3$, peaks s_4 and s_2 overlap each other, but the overlapping peak position is different from that in Fig.3(d). For peak s_2, a large enhancement is found due to the resonance mode coupling between the two clusters. When η increases to 1.6 in Fig.4(e) and 2.0 in Fig.4(f), peaks s_4, s_5, and s_6 are blueshifted and peak s_4 has a larger intensity than that shown in Figs.3(e) and 3(f), and the peaks s_1, s_2, and s_3 have a slight shift. In Figs.3 and 4, it is found that the coupling among the resonance modes of the two clusters tends to enhance the high peaks and weaken the low ones. Comparing with the domination of local dielectric resonances in the optical responses, we can conclude that the ambient perturbation is a very small modulation.

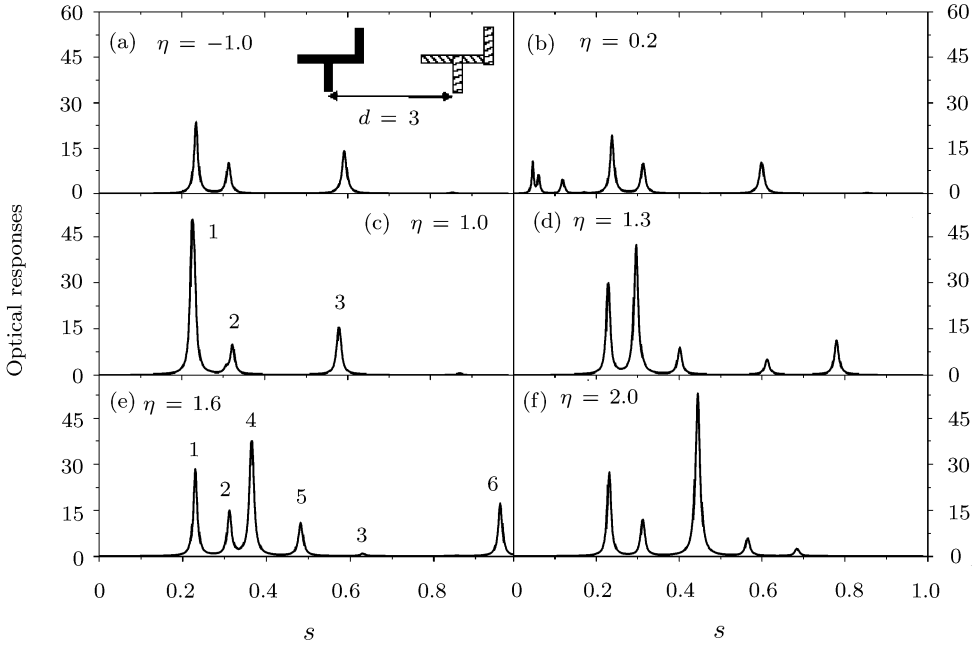


Fig.4. Optical responses of two close clusters with the distance $d = 3$. (a) $\eta = -1.0$, (b) $\eta = 0.2$, (c) $\eta = 1.0$, (d) $\eta = 1.3$, (e) $\eta = 1.6$, and (f) $\eta = 2.0$.

For more details, local field distributions of the two clusters near resonances are plotted in Fig.5. For simplicity, only $\eta = 1.0$ is considered. Figure 5(a) displays the residue of electric potentials near resonance $s_1 = 0.22469$ with $d = 3$, while Fig.5(b) displays the residue of electric potentials near $s_1 = 0.23739$ with $d = 10$. For the two closely situated clusters, the fields are more localized within and around these two clusters, showing a collective response.[14] However, when the two clusters are separated farther away, there is little correlation between their field distributions. Therefore, the collective response of local fields leads to stronger optical responses.

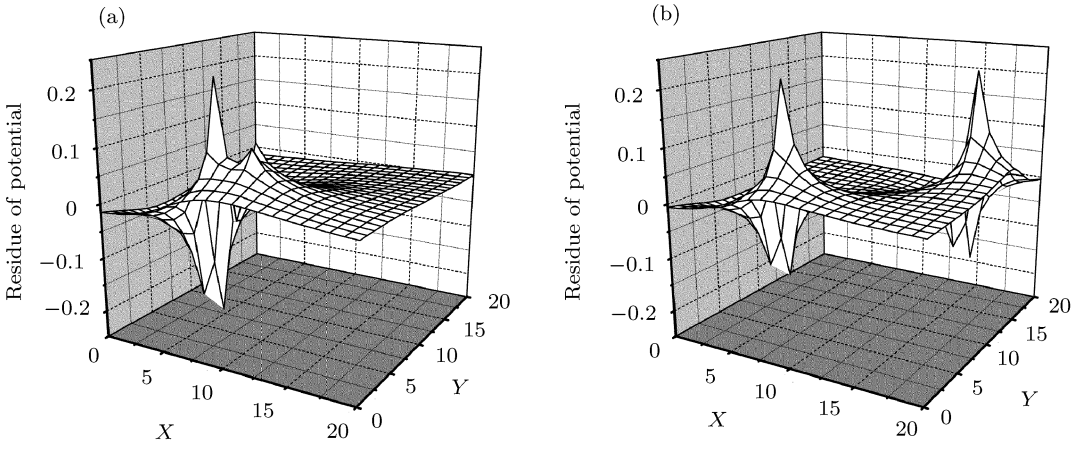


Fig.5. Local field distributions near resonances for two kinds of clusters in Figs.3 and 4. Here $\eta = 1$. (a) The residue of electric potentials near resonance $s_1 = 0.22469$ with $d = 3$. (b) The residue of electric potentials near $s_1 = 0.23739$ with $d = 10$.

In Figs.3 and 4, through increasing the admittance of metallic component, the absorption peaks are enhanced and blueshifted. In practical applications one would like to find large optical responses within the infrared region. It is known that the optical responses will be redshifted if we increase the size of bonds in the cluster. An explanation about this is given here. If a wavelength λ is to be found corresponding to one of the resonances of the cluster for some size c, then when we enlarge the size to $2c$, this resonance should happen at the wavelength of 2λ. Consequently, the frequency becomes $\omega/2$ and the peak is redshifted. Figure 7 displays the redshift of optical responses corresponding to the clusters in Fig.6. We find that all the absorption peaks are redshifted with the increase of cluster size.

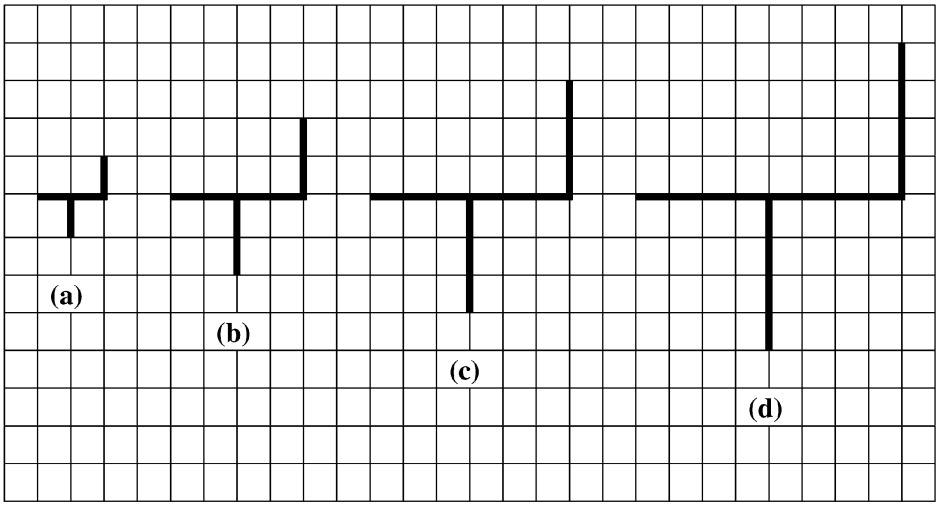


Fig.6. Schematic diagram of metallic clusters with similar geometry, but different sizes.

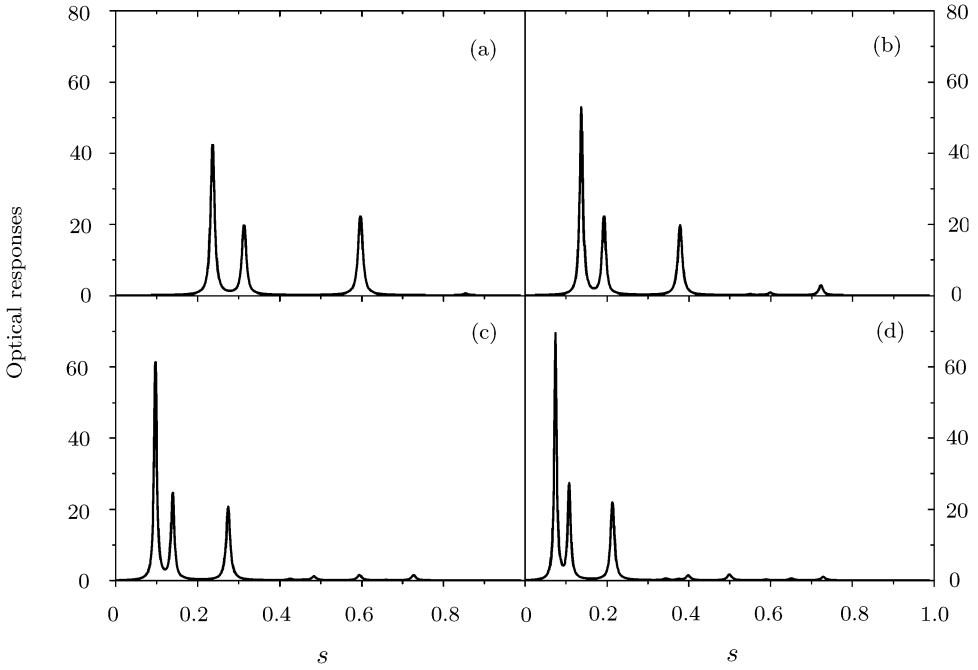


Fig.7. The optical responses of the metallic clusters with different sizes corresponding to Fig.6.

Besides the ways for controlling the optical responses mentioned above, we find that the main peak of an absorption spectrum is determined by the bonds parallel to the applied field. If the bonds along the applied field increase, then the main peaks will redshift just as found in Fig.7, while the bonds perpendicular to the applied field will cause the birth of subpeaks. By changing the length of these bonds, we can modulate the strengths of the corresponding peaks. This may provide us the way to control the optical response by modifying the geometry of the clusters.

Since the optical responses of lattice animals have been calculated in Table 1, by assigning the different lattice animals into the dilute composites, we can design the optical responses we desire to have. According to the dielectric local resonance mechanism, we can obtain the blueshifted optical responses with the increase of η. Meanwhile, by increasing the size of the metallic cluster, the optical responses are greatly redshifted. To summarize, by means of modulating the ratio η, the geometry, the cluster size and the admittance of metallic clusters, we can effectively control the optical responses of dilute composites.

5. Summary

In this paper, we have shown that the optical responses in the dilute composites can be controlled through considering the local dielectric resonance mechanism. we have deduced the effective linear optical responses of three-component composite

$$\varepsilon_{\rm e} = \varepsilon_0\Big(1 + \sum_{n=1}^{n_{\rm s}} \frac{\gamma_n}{\varepsilon_0(s - s_n)}\Big),$$

and the sum rule of cross sections:

$$\sum_{n=1}^{n_i} (\gamma_{n_1} + \eta\gamma_{n_2}) = N_{h_1} + \eta N_{h_2},$$

in which N_{h_1} and N_{h_2} are the numbers of ε_1 and ε_2 bonds along the applied electric field, respectively. For the design of optical properties, the cross sections (which are used to represent the strengths of optical responses) for various lattice animals were computed. By comparing two sets of clusters ($d = 10$ and $d = 3$), we find that the local resonance determines the main optical responses, while the ambient perturbation only has a small contribution. When $\eta[= (\varepsilon_2 - \varepsilon_0)/(\varepsilon_1 - \varepsilon_0)]$ is positive and increases, there exists the blueshift of absorption peaks. On the other hand, the absorption peaks will be redshifted by enlarging the cluster size. By considering the ratios of the metallic clusters to the whole composite, their geometry, size and admittances of the nanometre metallic clusters in the dilute composites, we can control the positions and intensities of absorption peaks effectively. These results may be beneficial to the study of surface plasmon resonances on a nanometre scale.

References

[1] See article in 1997 *Nanostructured Materials: Clusters, Composites and Thin Films*, edited by Shalaev V M, ACS Symposium Series 679 (Washington D C, American Chemical Society)

[2] Stockman M I 2000 *Phys. Rev.* B **62** 10494

[3] Gu Y and Yu K W 1999 *Phys. Rev.* B **59** 20

[4] Dai B, Gu Y, Li C and Gong Q H 2004 *Eur. Phys. J.* B **42** 165

[5] Markel V A, Shalaev V M, Zhang P, Huynh W, Tay L, Haslett T L and Moskovits M 1999 *Phys. Rev.* B **59** 10903

[6] Sarychev A K, Shubin V A and Shalaev V M 1999 *Phys. Rev.* B **60** 16389

[7] Stockman M I, Faleev S V and Bergman D J 2001 *Phys. Rev. Lett.* **87** 167401

[8] Safonov V P, Shalaev V M, Markel V A, Danilova Y E, Lepeshkin N N, Kim W, Rautian S G and Armstrong R L 1998 *Phys. Rev. Lett.* **80** 1102

[9] Ozbay E 2006 *Science* **311** 13

[10] Kik P G, Maier S A and Atwater H A 2004 *Phys. Rev.* B **69** 045418

[11] Gu Y and Yu Kin-Wah 2002 *Chin. Phys.* **11** 601

[12] Gu Y and Gong Q H 2004 *Phys. Rev.* B **70** 092101

[13] Dai B, Gu Y, Li Chen and Gong Q H 2005 *Phys. Rev.* B **72** 064112

[14] Wang L J, Gu Y, Dai B and Gong Q H 2006 *J. Phys: Condens. Matter* **18** 4515

[15] Wang Z W, Wang X F, Liu C L, Zhao X J, Xiang H, Yu J G, Gong Q H and Gu S X 2005 *Chin. Phys.* **14** 551

[16] Diao J J, Chen G D, Xi C, Fan Z Y and Yuan J S 2003 *Chin. Phys.* **12** 100

[17] Gu Y and Gong Q H 2003 *Phys. Rev.* B **67** 014209

[18] Bergman D J and Stroud D 1992 *Solid State Physics* **46** 147

[19] Bergman D J 1978 *Phys. Rep.* **43** 377

[20] Clerc J P, Giraud G, Luck J M and Robin Th 1996 *J. Phys.* A: *Math. Gen.* **29** 4781